specific. However, our results indicate that both adaptations may occur in the same species, with streamside *Spartina* utilizing the first type and the inland form utilizing the second.

In the streamside zone, at soil redox potentials (+200 mV) indicating moderate reduction, root respiration was primarily aerobic, as evidenced by the high ATP levels and low ADH activity (Fig. 1, c and d). As the soil redox potential became more negative within the streamside zone, malate concentrations significantly increased while ADH activity remained low (Fig. 1c), indicating that in the absence of alcoholic fermentation the possible importance of malate in the metabolic adjustment of the plant to anaerobiosis. The ATP concentration and energy charge ratio decreased because there was no net ATP synthesis. The second type of adaptation was operative in the inland zone where soil redox potentials were low, ADH activity was induced, and ethanol was the primary end product of anaerobic respiration but was lost through diffusion from the roots; the energy supply was maintained by an increased rate of glycolysis (Fig. 1, c and d).

The specific metabolic adaptation to anoxia used by *Spartina* appears to be environmentally induced by the intensity of soil reduction. In contrast to what has been previously thought, the aerenchyma tissue in *Spartina* does not conduct sufficient oxygen to the roots for complete aerobic respiration in highly reduced substrates. Therefore, hydrological modifications of salt marshes that cause increased soil waterlogging may affect root respiration and, ultimately, plant productivity.

I. A. MENDELSSOHN
K. L. MCKEE
W. H. PATRICK, JR.
*Laboratory for Wetland Soils and Sediments, Center for Wetland Resources, Louisiana State University, Baton Rouge 70803*

### References and Notes

1. *Spartina alterniflora*, the dominant angiosperm in regularly flooded salt marshes of the Atlantic and Gulf coasts of the United States, often occurs as relatively distinct height forms along a complex gradient of environmental factors landward from tidal creek banks. Along the Louisiana Gulf Coast, this gradient in *Spartina* productivity is identified by two forms: a high vigor streamside (~1 m) form and a low vigor inland (60 to 80 cm) form. However, the low vigor inland form often grades into an even less vigorous form (< 50 cm) whose habitat is characterized by small open bodies of water, continuous flooding, and *Spartina* dieback [W. G. Smith, *Coastal Stud. Bull.* **5**, 89 (1970)].
2. J. M. Teal and J. W. Kanwisher, *J. Exp. Bot.* **17**, 355 (1966).
3. C. D. John and H. Greenway, *Aust. J. Plant Physiol.* **3**, 325 (1976).
4. Ethanol and malate were determined by the methods of H. U. Bergmeyer, *Methods of Enzymatic Analysis* (Academic Press, New York, 1963), pp. 285 and 328.
5. R. M. M. Crawford, *J. Exp. Bot.* **18**, 458 (1967); ——— and M. McMannon, *ibid.* **19**, 435 (1968).
6. I. A. Mendelssohn and K. L. McKee, *Aquat. Bot.*, in press.
7. D. E. Atkinson, *Biochemistry* **7**, 4030 (1968).
8. The potential of a calomel electrode against a standard hydrogen electrode (+244 mV) was added to the measured potential to calculate $E_h$.
9. L. R. Gardner, *Southeast. Geol.* **15**, 17 (1973); I. A. Mendelssohn and E. D. Seneca, *Estuarine Coastal Mar. Sci.* **11**, 27 (1980).
10. D. D. Hook, C. L. Brown, P. P. Kormanik, *J. Exp. Bot.* **22**, 78 (1973).
11. I. A. Mendelssohn and M. T. Postek, *Am. J. Bot.*, in press.
12. R. M. M. Crawford, in *Nitrogen in the Environment*, D. Nielsen and J. G. McDonald, Eds. (Academic Press, New York, 1978), vol. 1, p. 427.
13. C. D. John, V. Limpinuntana, H. Greenway, *Aust. J. Plant Physiol.* **1**, 513 (1974); P. Raymond, F. Bruzau, A. Pradet, *C. R. Acad. Sci.* **286**, 1061 (1978).
14. A. Pradet and J. L. Bomsel, in *Plant Life in Anaerobic Environments*, D. D. Hook and R. M. M. Crawford, Eds. (Ann Arbor Science, Ann Arbor, Mich., 1978), p. 89.
15. H. A. Krebs, in *Essays in Biochemistry*, P. N. Campbell and F. Dicken, Eds. (Academic Press, New York, 1972), p. 1; H. Lambers, *Physiol. Plant.* **37**, 117 (1976).
16. J. R. Giurgevich and E. L. Dunn, *Oecologia (Berlin)* **43**, 139 (1979).
17. A. Bertani, I. Brambilla, F. Menegers, *J. Exp. Bot.* **31**, 325 (1980).
18. J. E. Keeley, *ibid.* **29**, 1345 (1978).
19. F. N. Ponnamperuna, *Adv. Agron.* **24**, 29 (1972).
20. R. M. M. Crawford, in *Plant Life in Anaerobic Environments*, D. D. Hook and R. M. M. Crawford, Eds. (Ann Arbor Science, Ann Arbor, Mich., 1978), p. 119.
21. We thank R. M. M. Crawford, M. Cohn, J. Keeley, and D. Longstreth for reviewing the manuscript. Supported by funds from the National Oceanic and Atmospheric Administration Office of Sea Grant.

16 September 1980; revised 19 December 1980

## Metals in Estuarine Sediments: Factor Analysis and Its Environmental Significance

Abstract. *Q-mode factor analysis has been used to partition the variability of environmentally active metals in Delaware Bay sediments. Three factors, identified as a natural background source, an oceanic or seawater source, and an estuarine source, account for 96 percent of the metal variability.*

Trace metals may enter an estuary in dissolved, colloidal, or suspended forms, but most seem to be associated with suspended particulate matter (*1*) which is distributed to an estuary by the hydrodynamics of the system. In a model case, then, there should be definite gradients in the properties of suspended and bottom sediments along the estuary. In practice, however, poorly understood secondary processes modify the properties of the suspended particles and bottom sediments to such an extent that physical or chemical gradients are rarely obvious. Factor analysis can be a valuable tool for the identification of important metal gradients of estuarine bottom sediments, providing insight into the overall processes responsible for these gradients and into the identification of bottom areas containing high concentrations of environmentally active and potentially toxic materials.

Applications of *Q*-mode factor analysis to geological problems have included the classification of Bahama Bank sediments, the analysis of heavy-mineral suites in the Gulf of California, the extraction of paleoclimatological information from microfossil assemblages in ocean sediments, and comparison of the chemistries of surface waters and country rock in river basins (*2*). The results of *Q*-mode factor analysis are written as two small matrices, the $F_s$-matrix and the *B*-matrix, the product matrix of which is an approximation of the original data matrix. The percentage of variance explained is a measure of the degree to which this product matrix approximates the original data matrix.

The data set consists of analyses of the fine-grained fraction (< 63 μm) for environmentally active (*3*) metals and particulate organic matter from Delaware Bay sediments. A wide range of concentrations occurred between and within the analyzed variables, even though the samples represent only the fine fraction of the bottom sediments from the central region of the Delaware estuary.

We have applied factor analysis to the data (*4*) on each of 18 variables from 119 samples. The analysis reveals that three factors account for 96 percent of the variance in the original matrix. The $F_s$-matrix (Table 1) is a listing of combinations of the 18 variables that define the compositional end-members for each of the three factors. Factor I is dominated by Fe, Mg, K, Li, and Al, and none of these five metals is strongly dominant over the others. Factor I accounted for 50.9 percent of the total variance in the data bank. Factor II is dominated by Sr, Mg, Ca, and Na and accounted for 24.1 percent of the total variance in the data bank. Factor III includes those metals usually considered to be potentially hazardous. It is dominated by Cu, Cr, Pb, Hg, and organic material, with some affinity shown by Cd, Ni, Zn, and Fe. Factor III accounted for 21 percent of the total data variance.

The *B*-matrix is a matrix of weights or loadings for each of the factors at each


0036-8075/81/1023-0441$01.00/0  

sampling point—in this case, the influence exerted by each end-member on the total metal suite found in each sediment sample. We have plotted the distribution of *B*-matrix values for each station and for each factor. Figure 1A is a contour map illustrating the distribution of factor I (Fe, Mg, K, Al, and Li). Areas where the *B*-matrix values for factor I are greatest are places known to be sites where Holocene marsh sediments are exposed on the present floor of the bay (*5*), and the lowest value areas coincide with bottom types whose origin is thought to result from landward transport of continental shelf sediments in the bottom water layer of tidal waters (*6*). Highest values for factor II (Sr, Mg, Ca, and Na) occur in the most seaward reach of the study area and decrease regularly up the estuary (Fig. 1B). Values are higher on the New Jersey side than for laterally equivalent areas on the Delaware side of the bay. High *B*-matrix values for factor III (Cu, Cr, Hg, Pb, and organic matter) are found in the upper reaches of the study area with low values at the most seaward sites, although high values extend seaward along the Delaware side of the estuary.

On the basis of the chemical elements associated with each factor, the relative importance of each factor in the estuary, and knowledge of general circulation and sedimentation patterns in estuaries, some inferences on the identities of the three factors can be drawn. We interpret factor I to be representative of the terrigenous background level of these metals. The acid-soluble clay mineral chlorite in Delaware Bay sediments is composed of at least Fe, Mg, K, and Al, with Li serving as a possible charge-balancing lattice substituent. In addition, amorphous grain coatings contain Fe and Al as oxyhydroxides. Regions of the estuary where the influence of factor I is greatest are known to be sites where old marsh surfaces are exposed on the bay bottom or are upstream areas. Areas where factor I has the least influence coincide with areas whose sediment source is from the continental shelf. We associate factor II with the signature of seawater cations imposed upon sediments of the bay. A significant linear correlation between Sr in the fine fraction of bottom sediments and mean bottom water salinity supports this explanation. The influence of factor II is greatest on the sediments of the lower estuary and is consistent with the Coriolis-induced circulation pattern, causing oceanic effects to be greatest on the left side of the estuary (looking seaward) and terrigenous effects to be greatest on the right side. Highest values for factor III occur on the right side of the estuary, consistent with a river source of suspended sediments (*7*). The area of rapid decline for factor III corresponds to the downstream terminus of the submerged estuarine delta of the Delaware (*5*).

We cannot tell whether or how much factor III is associated with upstream pollution, but factor analysis, as used on this data set, demonstrates where metals associated with fine-grained sediment will accumulate on the bottom. Thus, factor analysis may be of great value in identifying the estuarine areas that might be influenced by upstream pollution. In

Table 1. Factor score ($F_s$) matrix, which relates the intensity of correlation between the three factors (these factors account for 96 percent of the variance) and the metals. The dominant metals within each factor group are indicated by asterisks.

| Metal | Factor I | Factor II | Factor III |
|---|---|---|---|
| Fe | 1.741* | 0.065 | 0.803 |
| Mg | 1.987* | 1.570* | −0.608 |
| Zn | −0.341 | 0.147 | 0.803 |
| Cr | 0.143 | 0.754 | 1.724* |
| Cu | −0.777 | 0.252 | 2.270* |
| Pb | −0.431 | 0.053 | 1.392* |
| Hg | −0.356 | 0.320 | 1.173* |
| Cd | −0.228 | 0.657 | 0.888 |
| Ni | 0.146 | −0.056 | 0.873 |
| Sr | −0.706 | 2.360* | −0.412 |
| Mn | −0.310 | 0.034 | 0.579 |
| Ca | −0.673 | 2.600* | −0.777 |
| Li | 1.779* | −0.200 | 0.171 |
| K | 1.632* | 0.247 | 0.359 |
| Al | 1.557* | −0.110 | 0.276 |
| Na | 0.164 | 1.111* | 0.166 |
| Si | 0.747 | 0.711 | 0.894 |
| Organic matter | 0.093 | 0.393 | 1.085* |

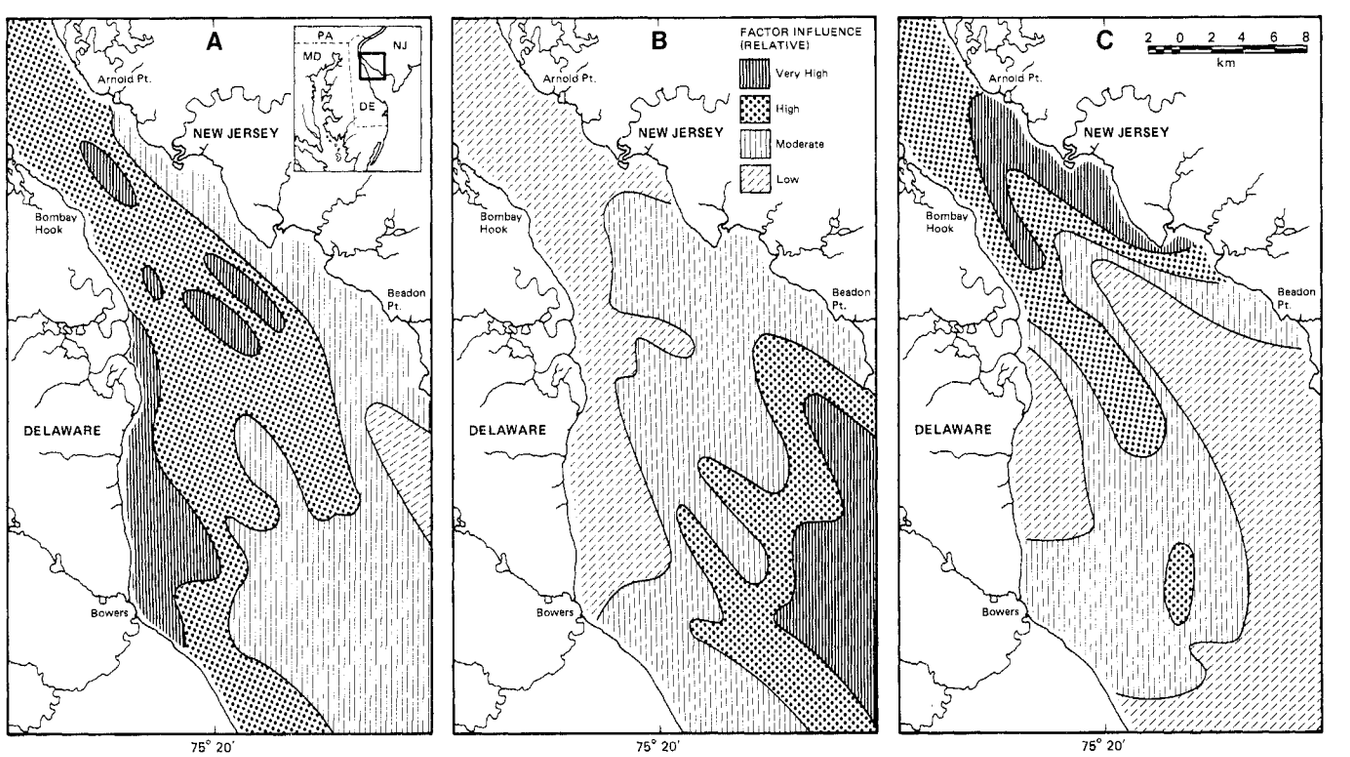


Fig. 1. *B*-matrix weights for each factor at each sampling point ($N$ = 119). (A) Relative influence of factor I (Fe, Mg, Li, K, and Al). (B) Relative influence of factor II (Mg, Sr, Ca, and Na). (C) Relative influence of factor III (Cr, Cu, Pb, Hg, and organic matter).

addition, it may enable fisheries managers to identify bottom areas containing high concentrations of environmentally active and potentially toxic materials, which may require careful scrutiny, particularly for harvesting benthic or demersal organisms.

FREDERICK BOPP III
*Roy F. Weston, Inc.,*
*West Chester, Pennsylvania 19380*
ROBERT B. BIGGS
*College of Marine Studies,*
*University of Delaware, Newark 19711*

### References and Notes

1. R. J. Gibbs, *Science* **180**, 71 (1973).
2. W. Krumbein and F. Graybill, *An Introduction to Statistical Models in Geology* (McGraw-Hill, New York, 1965); R. Miller and J. Kahn, *Statistical Analysis in the Geological Sciences* (Wiley, New York, 1962); J. Imbrie and E. Purdy, *Mem. Am. Assoc. Pet. Geol. 1* (1962); J. Imbrie and T. Van Andel, *Geol. Soc. Am. Bull.* **75**, 1131 (1954); J. Kovan and J. Imbrie, *Math. Geol.* **3**, 61 (1971); J. Imbrie and N. Kipp, in *Late Cenozoic Glacial Ages*, K. Turekian, Ed. (Yale Univ. Press, New Haven, Conn., 1971), p. 71.
3. Environmentally active trace metals are defined to be those cations that can be separated from the silt and clay fraction of the dried and disaggregated sediment by leaching with 10 percent hydrochloric acid at 70°C for 96 hours. Metals that are so firmly bonded to, or exchanged within, mineral grains that it is not possible to remove them under natural biochemical conditions are not considered. The laboratory extraction procedure used is designed to approximate, however crudely, the severest conceivable naturally occurring biochemical conditions without completely degrading the sediments and to reflect metals that are available for introduction to the marine food web through biological or chemical processes.
4. The raw data are contained in F. Bopp, master's (1973) and doctoral (1980) theses, University of Delaware. Because of the wide range in concentrations of the original variables, a data transformation was accomplished. The transformation, to the percentage of the maximum value for each variable, does not alter the accuracy of the factor analysis, since relative proportions and hence, locations of variance, are preserved.
5. C. Weil, *Del. Sea Grant Publ. 4-77* (1977).
6. J. Neilheisel, thesis, Georgia Institute of Technology (1973).
7. V. Klemas, M. Otley, W. Philpot, C. Wethe, R. Rogers, N. Shah, in *Proceedings of the 9th International Symposium on Remote Sensing of Environment* (Environmental Research Institute of Michigan, Ann Arbor, 1975), pp. 1289–1318.
8. Supported in part by the Sea Grant Program, grant 2-35223.

18 March 1981; revised 15 July 1981

## Epifluorescence and Video Analysis of Vacuole Motility and Development in Stomatal Cells of *Allium*

Abstract. *The vacuole in stomatal cells of* Allium *undergoes major changes in shape during differentiation, switching from a globular form in new guard mother cells to a network of interconnected tubules and chambers, and then back to a globular form as guard cells mature. In addition, vacuolar network elements exhibit characteristic movements and rearrangements.*

The vacuole of plants is an organelle whose functions in cell metabolism are only beginning to be appreciated (*1*). These structures are important in photosynthesis, lysis, osmoregulation, storage, seed germination, and generation of the turgor force necessary for cell expansion. Recent advances in the isolation of vacuoles are making it possible to characterize vacuole content as well as the proteins present in the tonoplast membrane (*2*). However, despite these advances in our understanding of vacuole physiology, comparatively little is known about the development, distribution, and movement of vacuoles. Marked changes in the size and position of vacuoles occur during cell growth and differentiation. In addition, changes in vacuole morphology accompany cyclic alterations in turgor in the motor cells of leaf pulvini (*3*). Available evidence indicates that vacuoles are formed from the endoplasmic reticulum, possibly through a pathway involving GERL [Golgi-associated endoplasmic reticulum from which lysosomes form (*1*, *4*)]. It has been proposed that the provacuoles that arise from this pathway constitute a network of tubular elements which coalesce to form the large central vacuole of the cell (*4*). In this report, we demonstrate vacuole motility and morphogenesis in living guard mother cells (GMC's) and guard cells of *Allium cepa* and *A. vineale*. Stomatal cells in this genus are advantageous for study because their vacuoles autofluoresce when excited with blue light (*5*). Because the vacuole stands out against the dark background of the remainder of the cell during fluorescence viewing, its organization can be more readily studied under these conditions than with phase or differential interference contrast (DIC) optics. Visualization, analysis, and archiving of fluorescence images are aided by the use of low-light-level television cameras and ancillary video equipment (*6*).

Mature guard cells in epidermal slices of *Allium* (*7*) contain large globular vacuoles located at either end of the cell and around the nucleus (Fig. 1d). The vacuole autofluoresces in the green region of the spectrum when it is excited with blue light. Emission spectra obtained with a microspectrophotometer mounted on the microscope (*8*) show a peak at 525 nm, a value similar to that previously reported (*5*).

When epidermal slices are prepared from the meristem region of cotyledons and leaves, early stages in stomatal differentiation can be examined. These observations show that vacuoles are present in the distal regions of protodermal cells undergoing asymmetric division, as well as in newly formed GMC's derived from these cells. In the latter the vacuoles are globular in shape, as judged by critical focusing with DIC optics. However, none of these vacuoles are autofluorescent. Instead, fluorescence appears in somewhat older GMC's located in more distal portions of the meristem (Fig. 1a). That the vacuole is still globular in form is evident from the fluorescence images (Fig. 1a). Fluorescence emission spectra from these young vacuoles are nearly identical to those of mature guard cells (*6*).

As the GMC's increase in size, the shape of the vacuole drastically changes. The organelle is transformed from the globular form seen earlier to a complex network or reticulum of interlinked tubules and small chambers (Fig. 1, e to j). The diameter of these elements is variable, and some as narrow as 0.1 to 0.5 μm have been seen (Fig. 1, i and j). The appearance of the network also varies from cell to cell. A GMC with a fine tubular network can exist close to another with many small spherical chambers. Careful focusing while viewing the video monitor, however, demonstrates that many if not all of the vacuole elements are interconnected.

The network is not an artifact. It is found in epidermal slices gently prepared to avoid cell damage. It is also present in GMC's located adjacent to mature guard cells that contain a globular system. Although the network is visible under fluorescence conditions, it is not evident with phase or even DIC optics. However, the reticulate nature of the vacuole was confirmed in the electron microscope with 0.5-μm-thick serial sections viewed at 100 kV (*9*).

The vacuole remains segmented in appearance during GMC division, so that each daughter guard cell receives its own network complement. The network is retained during the early stages of guard cell differentiation (Fig. 1b), but as the cells mature it is transformed back into large globules similar in form to those seen in very young GMC's and in mature guard cells. The globules are principally located at either end of the cell, but critical focusing indicates that they are interconnected by finer elements (Fig. 1c). The vacuole continues to grow in


0036-8075/81/1023-0443S01.00/0 